An experiment of spectral induced polarization

Roberto Balia([1]), **Gian Piero Deidda**([1]), **Alberto Godio**([2]), **Gaetano Ranieri**([2]), **Luigi Sambuelli**([2]) **and Giovanni Santarato**([3])

([1]) *Dipartimento di Ingegneria del Territorio, Università di Cagliari, Italy*
([2]) *Dipartimento di Georisorse e Territorio, Politecnico di Torino, Italy*
([3]) *Istituto di Mineralogia, Università di Ferrara, Italy*

Abstract
A Spectral Induced Polarization (SIP) survey was carried out in a mining test site in Sardinia (Italy). Measurements were developed along a profile by using an axial dipole-dipole array with 10 AB positions and 6 MN positions for each AB. The amplitude and phase spectra of the apparent resistivity were acquired in the 0.25-4096 Hz frequency range. The results obtained through the processing and inversion step seem to confirm that, with respect to the classical TD/FD Induced Polarization, SIP allows better discrimination of some important characteristics of mineral deposits such as mineral content and grain size.

Key words *mining – geophysics*

1. Introduction

Induced Polarization (IP) has been utilized in the largest number of applications and it has been the most successful in mining exploration, particularly in the search for metal oxide and sulphide mineralizations. In general the classical parameters of the method, *i.e.* chargeability for measurements carried out in Time Domain (TD) and frequency effect for those in Frequency Domain (FD), have contributed significantly to the definition of mineral ore bodies.

The IP methods can actually afford «finer» parameters than the classical ones, directly related to the characteristics of the dispersion of electric resistivity with frequency. The acquisition of the dispersion curve, in other words the resistivity spectrum, is at the basis of the method called «Spectral Induced Polarization» (SIP). Since the 1960's various authors have considered examining the spectral parameters at least from an experimental point of view (*e.g.* Pelton *et al.*, 1972). Among the various models proposed to express the relation between dispersion of resistivity and frequency, the so-called Cole-Cole model (Cole and Cole, 1941) has been the most widely used.

More recently Pelton *et al.* (1978) gave a very accurate study of SIP with both field and laboratory measurements on natural and synthetic mineralized samples. In this study the characteristics of the spectral parameters were outlined as well as their possible associations with important economic parameters such as the grain size and the mineral content. The study concerned a SIP experiment in a well known mining site: the gold-bearing deposit of Serrenti-Furtei (South Sardinia – Italy).

2. Geological outline

The Oligo-Miocene volcanic cycle was characterized by two phases: a volcanic fissure phase with discharge of calc-alkaline lavas and a subsequent phase with highly explosive and effusive eruptions. This volcanic cycle is very

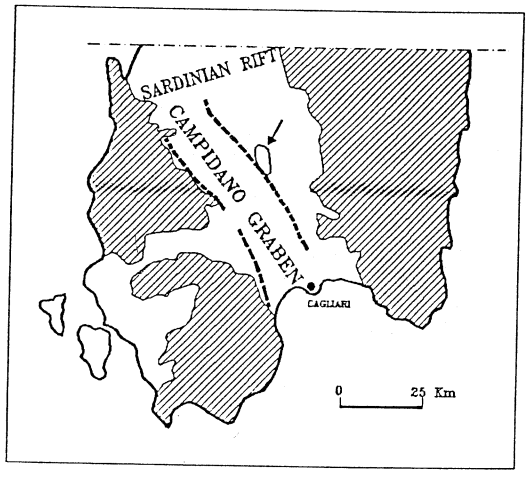

Fig. 1. Geological sketch map of Southern Sardinia. Dashed areas correspond to Paleozoic horsts and white areas to Tertiary and Quaternary sediments and volcanites. The arrow indicates the outcrop of Oligo-Miocene volcanites that includes gold-bearing mineralizations.

important in that a minerogenetic event with deposition of metal minerals and precious metals is attributable to the associated epithermal phenomena. Figure 1 is a schematic representation of the geology of Southern Sardinia with the main structural elements: the Paleozoic basement dismembered in different horsts, the Sardinian rift and the Campidano graben. The Oligo-Miocene volcanites that constitute the study area outcrop close to the eastern border of the Campidano graben, at about 40 km north of the town of Cagliari, between the villages of Serrenti and Furtei. The main body of the outcrop is approximately elliptical with axes of about 7 and 5 km respectively (Grillo *et al.*, 1990). It includes economically feasible gold-bearing mineralizations.

The epithermal mineralizations related to the Oligo-Miocene cycle are usually divided into two categories: the high sulphidation type and the low sulphidation type. The Serrenti-Furtei mineralizations belong to the first type and are generally associated with enargite, pyrite, calcopyrite and vuggy silica. Figure 2 shows qualitatively the ways of deposition and the relations between main mineralization and host rock: the volcanic explosion gives rise to a diatreme which also includes andesite blocks. The mineral is deposited at the diatreme-andesite contact by hydrothermal activity.

Figure 3 shows a schematic geological map of the study area and the position of the measurements' profile. While pyrite occurs in the diffused state over the entire environment, enargite and the gold-bearing mineralizations occur only with the diatreme, particularly where it shows alteration with vuggy silica. However, pyrite here is not present in the same way as in the host rock, especially because the grain size increases and in some places reaches the massive state.

Because of these relatively complex characteristics of the mineralization, with polarizable species both inside and outside the strip of interest but with substantial differences in grain size and texture characteristics, and because of the presence of different substances such as enargite and gold, the site was considered a challenging opportunity to test SIP and its potential.

3. Field measurements

Field measurements were carried out using a model IPT1 transmitter and a model V4T receiver, both from Phoenix Geophysics Ltd. This equipment allows readings directly in the field of both amplitude and phase data. The measurements were developed on 10 positions of AB and 6 positions of MN for each AB. Since in our case AB = MN = 10 m, the total length of the profile was 170 m.

Three experimental pseudosections were constructed (fig 4a-c) following classical definitions of apparent resistivity, percent frequency effect (PFE) and phase at 1 Hz. The apparent resistivity pseudosection was drawn by resorting to 0.25 Hz amplitude data, while the PFE one was drawn using as low and high frequency resistivities the amplitudes at 0.25 and 8 Hz respectively. The available high frequency information was ignored at this stage mainly to interpret the buried structure by means of a set of low frequency data.

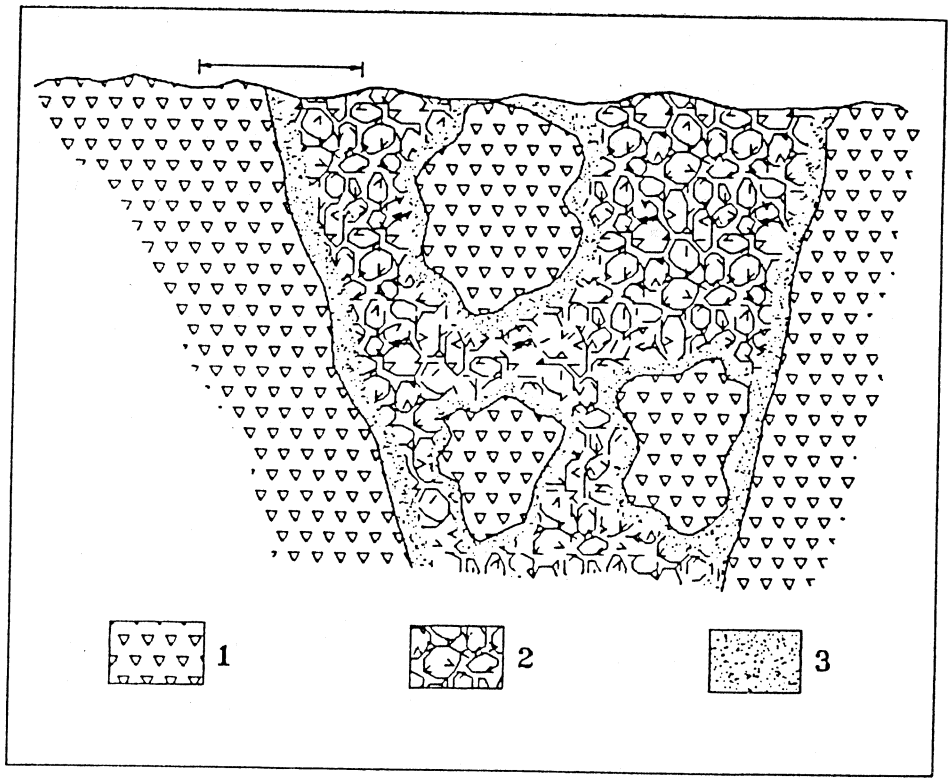

Fig. 2. Qualitative sketch section of an epithermal mineralized area. 1: Andesites and andesite blocks; 2: diatremic breccia; 3: areas of mineral deposition. The line in the upper part shows the relative scale of survey.

The pseudosection of apparent resistivity (fig. 4a) is characterized by two strong, limited resistive shallow anomalies, west of the outcrop of the orebody, while the rest fluctuates between 15 and 40 Ohm.m. The pseudosections of IP (fig. 4b,c) look substantially the same; they both have a strong central positive anomaly in a field of values that decreases gradually towards the extreme parts of the section and the isolines of both pseudosections present a trend that typically depends on the type of array used, while there is no trace of anomaly corresponding to the surface anomalies in the pseudosection of apparent resistivity.

4. Interpretation of the pseudosections

The pseudosections of apparent resistivity and of apparent PFE were interpreted in terms of two-dimensional modelling with a trial and error procedure. After several trials, the two-dimensional model that best fitted the experimental data proved to be the one reported in fig. 4a-c. It consists of a homogeneous half-space with a resistivity of 35 Ohm·m and 3% PFE, where 3 irregular bodies are included. The three resistive shallow bodies (180 Ohm.m) were attributed a PFE of 5%, while the central body is conductive (15 Ohm·m) and polarizable (18% PFE). Identification of this

body as the mining target is quite obvious, while the shallow resistive bodies can be associated with the outcrops of massive andesite bordering the orebody, although the easternmost of these bodies seems uncorrelated with respect to the surface geology (fig. 3). The gold-bearing orebody was therefore successfully identified within a mineralized matrix both because the geoelectrical and IP data proved to be complementary and because of the unexpected PFE contrast between the mineralized orebody and the surrounding matrix which itself contains pyrite and therefore can give a detectable IP response.

5. SIP data processing and interpretation

Amplitude and phase spectra of the apparent resistivity were obtained in each MN position in the above mentioned frequency band 0.25-4096 Hz: a total of 60 amplitude and phase spectra were thus available.

Signal-to-noise ratio was generally good, except several data at 256 Hz, most probably biased by the near notch filter at 250 Hz harmonics of mains.

Visual examination of phase spectra showed two main trends. The first kind of spectra shows low values at low frequencies and a re-

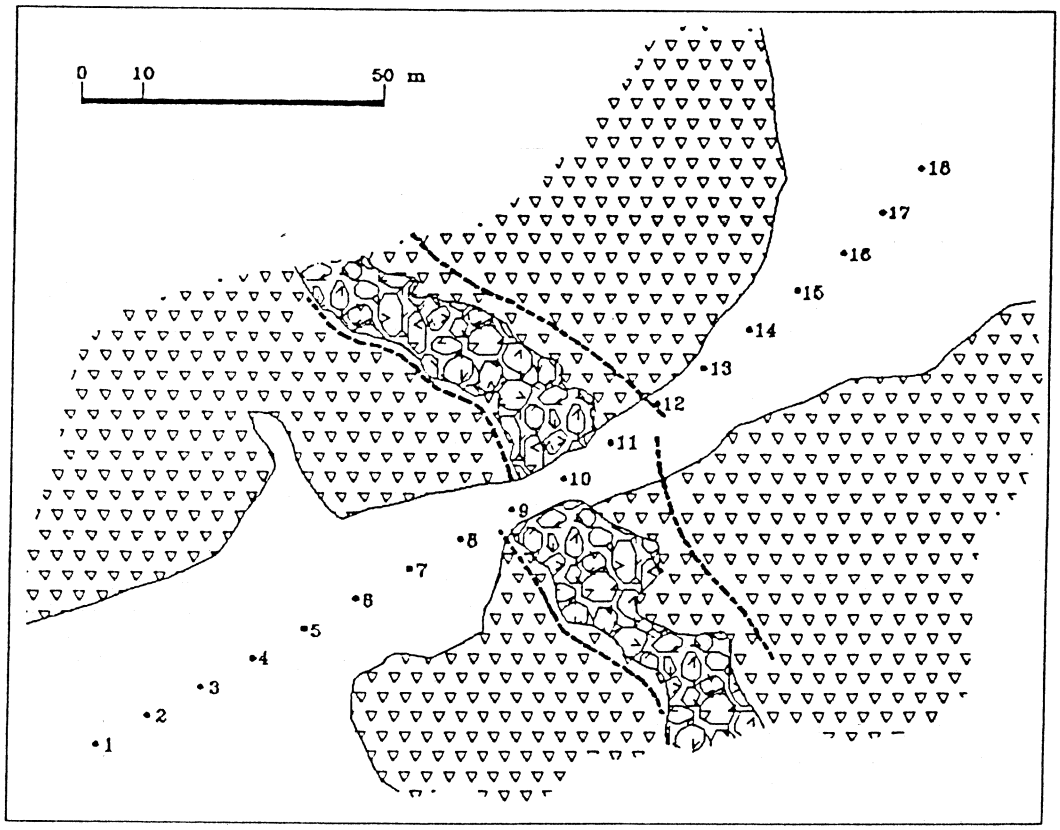

Fig. 3. Geological sketch map of the study area (for geological symbols refer to fig. 2). The dashed lines are the limits of the gold-bearing mineralization; numbered dots represent the electrode positions.

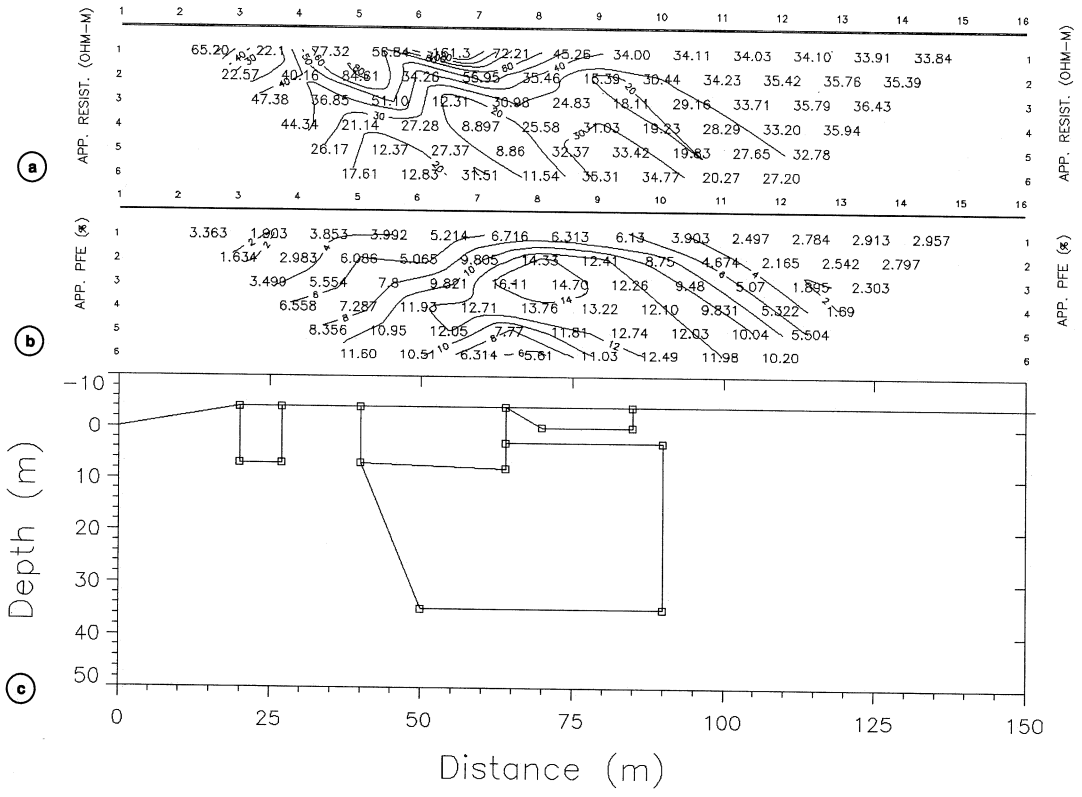

Fig. 4a-c. Best fit model and corresponding computed pseudosections of apparent resistivity and PFE.

markable increase at the highest frequencies, with a change of slope around 100 Hz; the second kind shows generally high values of the phase at low frequency and a gentler increase in values with increasing frequency. Two typical examples of both families are reported in fig. 5. The former kind was acquired, with some minor variations, everywhere, while the later kind of spectra was exclusively measured in few dipole-dipole layouts, around the mining target, *i.e.* for AB = 4 to 7 and n = 2 to 4. It is quite obvious that the former spectra are the response of the host rock, while the latter are strongly related to the embedded mining target.

5.1. *Inversion of amplitude and phase spectra*

The generally accepted interpretative model for quantitative description of SIP data is, as mentioned in the introduction, the Cole-Cole relaxation model (Cole and Cole, 1941):

$$Z(\omega) = R_0\left[1 - m \cdot \frac{1}{1 + (i\omega\tau)^c}\right] \qquad (5.1)$$

where $Z(\omega)$ (Ohm) is the complex impedance, ω (rad/s) the angular frequency, R_0 (Ohm) the d.c. resistance of the medium (ohmic paths),

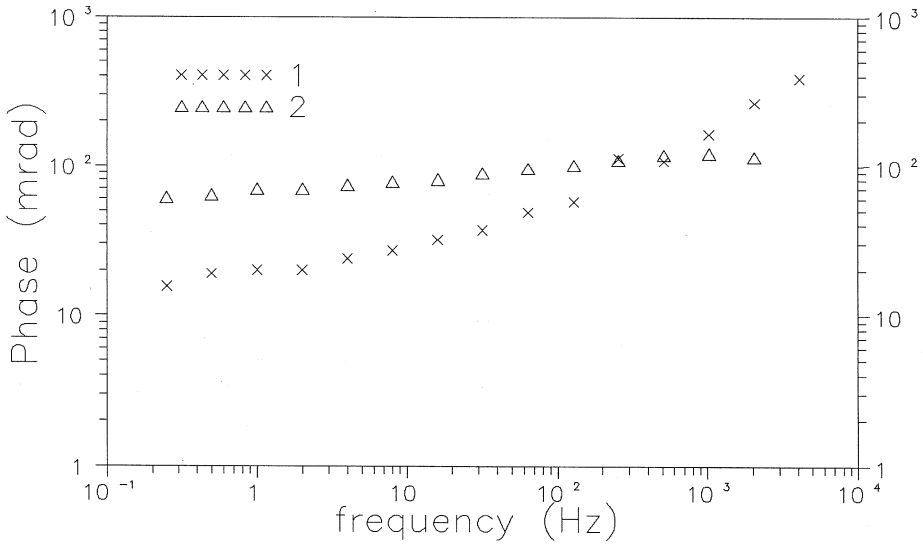

Fig. 5. Examples of field phase spectra; AB = 1, n = 3; AB = 5, n = 3.

m (ms) the chargeability, as defined by Seigel (1959), τ (s) the coefficient of relaxation and c the dispersion factor.

Briefly speaking, the m parameter mainly affects the phase maximum and the inflection slope of the amplitude, τ influences the position of the spectra with respect the frequency axis and c mainly governs the phase spectrum slope.

Given a couple of spectra, it is possible, by means of a non linear joint inversion of amplitude and phase, to determine the parameters of the best fitting Cole-Cole model. In turn it would be possible to draw pseudosections of the inverted parameters, whose correlation with the mineralogic and textural characters of the investigated structure should then be established (Johnson, 1984).

Taking advantage of the relatively simple geometry of the buried structure (see fig. 4a-c), it was preferred to follow an alternative approach, first suggested by Pelton *et al.* (1978). Under quite general hypotheses about the geometry and polarizability of both a host rock and an embedded polarizable body, Song and Vozoff (1985) showed that the following approximate relation holds:

$$Z_a(\omega) \approx Z_1(\omega)^{B_1(\omega)} \cdot Z_2(\omega)^{B_2(\omega)} \qquad (5.2)$$

where $Z_i(\omega) = \rho_i(\omega)/\rho_i(0)$ is the frequency-dependent impedance of the i-th medium and $Z_a(\omega) = \rho_a(\omega)/\rho_a(0)$ is the measured impedance. The frequency-dependent $B_i(\omega)$ are the well known «dilution factors», already defined by Seigel (1959) as

$$B_i = \frac{\partial \ln \rho_a}{\partial \ln \rho_i} \qquad (5.3a)$$

and the closure condition

$$\sum B_i = 1 \qquad (5.3b)$$

holds.

In equation (5.2) there are two unknown «true» spectra and two unknown (but correlated) B_i. Nevertheless, supposing that spectra pertaining to the first family (see the example reported in fig. 5), are the true spectra of the polarizable host rock, it is reduced to solving

for two unknowns, *i.e.* $Z_2(\omega)$ and $B_2(\omega)$ as (5.2) and (5.3a,b) give

$$Z_2(\omega) \approx [Z_a(\omega) \cdot Z_1(\omega)^{B_2(\omega)-1}]^{1/B_2(\omega)} \quad (5.4)$$

Now the spectra of the host rock cannot be fitted by a single Cole-Cole relaxation, due to the change in slope in the phase spectrum. A question may arise whether a multiplicative or additive combination of Cole-Cole relaxations should be preferred to fit the frequency-dependent complex resistivity of a polarizable medium. As pointed out by Major and Silic (1981) no valid physical reason exists for the choice; thus, in agreement with Pelton *et al.* (1978) and in view of comparing the results with theirs, the multiplicative combination was chosen:

$$Z(\omega) = R_0 \cdot [1 - m_1 f_1(\omega)] \cdot [1 - m_2 f_2(\omega)] \quad (5.5)$$

where

$$f(\omega) = 1 - \frac{1}{1 + (i\omega\tau)^c}$$

The joint inversion of the host rock amplitude and phase spectra was performed by means of the computer software NLSIP, kindly made available by Anderson (Anderson and Smith, 1986). The following results were obtained as mean values from several normalized spectra (fig 6):

$$R_0 = 1 \quad m_1 = 0.9 \quad \tau_1 = 0.000018 \quad c_1 = 0.7$$
$$m_2 = 0.14 \quad \tau_2 = 0.03 \quad c_2 = 0.3$$

Parameters with indices 1 and 2 respectively fit the high frequency and the low frequency parts of the spectra. Figure 6 reports the field spectra of layouts AB = 1, n = 3 and AB = 10, n = 3 as data examples together with the curves of calculated spectrum by using the above parameters.

The c_1 value, fairly less than 1, excludes

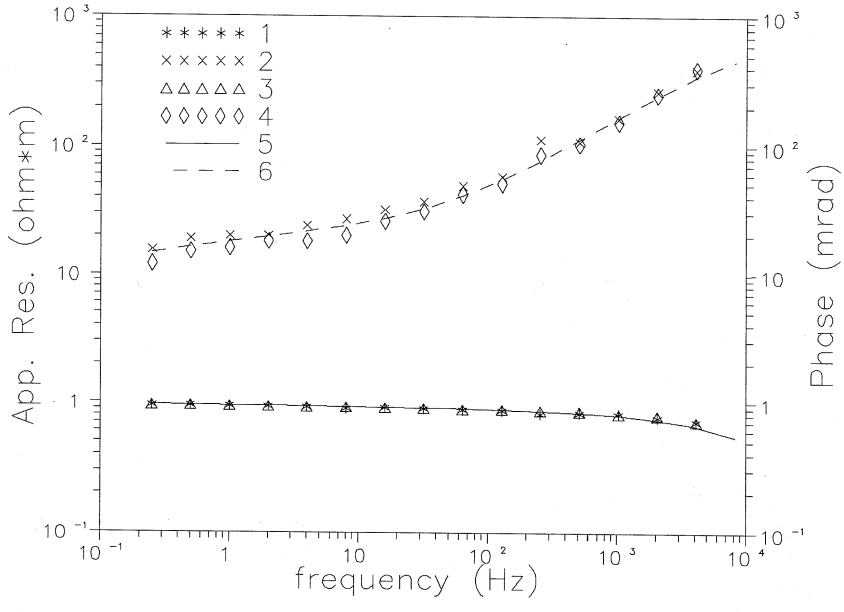

Fig. 6. Inversion of amplitude-phase spectra of host rock; 1 and 3: normalized amplitudes of respectively AB = 1, n = 3 and AB = 10, n = 3; 2 and 4: phases of respectively AB = 1, n = 3 and AB = 10, n = 3; 5 and 6: best fitting Cole-Cole normalized amplitude and phase responses of the host rock.

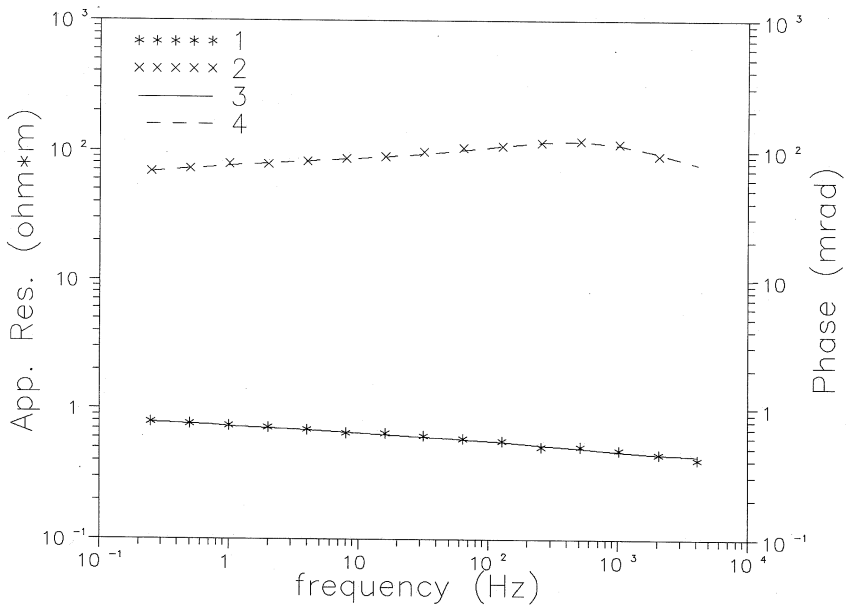

Fig. 7. Inversion of amplitude-phase spectra of the mining body; 1 and 2: normalized amplitude and phase of AB = 5, n = 3; 3 and 4: best fitting Cole-Cole normalized amplitude and phase responses of the mining body.

that the electromagnetic inductive coupling affects data even at the highest frequencies. Moreover the value of τ_1 can only be considered a rough estimate of its true value, as the abscissa of the maximum of phase spectrum is not enough constrained by the data; as a consequence the true value of τ_1 is most probably much lower.

In order to determine $B_2(\omega)$, the derivatives in definition (5.3a) were estimated by numerical modelling and differentiating the apparent resistivity response of the above defined geometry (fig. 4a-c) at all acquired frequencies, keeping of course the geometry fixed and varying resistivities of both host rock and anomalous body. For the layout whose phase spectrum is reported in fig. 5 (AB = 5, n = 3), a value for B_2 of about 0.85, approximately constant against frequency, was found. This finding strongly simplified estimating of the left side in (5.4), as

$$Z_2(\omega) \approx [Z_a(\omega) \cdot Z_1(\omega)^{B_2-1}]^{1/B_2} \qquad (5.6)$$

The frequency dependence of B_i's is dropped. After applying the correction in (5.6), the spectra of this layout, chosen as a representative of the family of spectra strongly perturbed by the polarizable body, were both modified. Again, a complex spectrum has to be inverted. Using the multiplicative combination of 2 Cole-Cole relaxations, we obtained by joint inversion the following estimates of the Cole-Cole model parameters (fig. 7):

$$R_0 = 1 \quad m_1 = 0.18 \quad \tau_1 = 0.0003 \quad c_1 = 0.7$$
$$m_2 = 0.55 \quad \tau_2 = 0.13 \quad c_2 = 0.25$$

A fair increase in τ_i values can be noted with respect to the background spectrum, together with remarkable variations in chargeability values.

6. Discussion

In order to interpret the results, it was found useful to consider the graph taken from Pelton

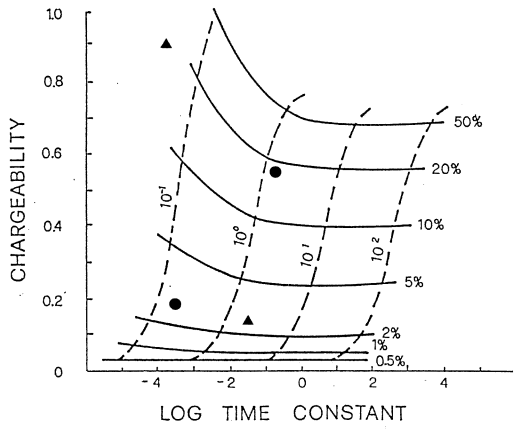

Fig. 8. Mineral discrimination nomogram (after Pelton *et al.*, 1978). Full and dotted lines represent respectively the lines of constant sulfide concentration (%) and of constant grain size (mm). Full triangles and circles correspond to the values of chargeability and time constant obtained by spectra inversion in fig. 6 (triangles) and 7 (circles).

et al. (1978) and reported in fig. 8. It is a nomogram constructed on a relevant number of experimental data collected from synthetic samples of sulphide mineralizations, which correlates Cole-Cole parameters τ and m with basic properties of the mineralization, such as the grain size and the mineral content. The four couples of parameters m and τ inferred from the inversion locate the points reported in the graph. The position of the four experimental points in the nomogram therefore seems to suggest that in the host rock (*i.e.* with AB = 1, n = 3) the mineral is present with a certain content (that can be estimated at most 10-20% by extrapolating the curves) and fine grained, while the larger grain size is present in a much lower percentage (about 2%). On the other hand when analyzing the mineralized area of economic interest (*i.e.* with AB = 5, n = 3), it can be seen that the content of the fine-grained mineral is practically unchanged, while the larger grain size mineralization is significantly increased both in volume (about 18%) and in size.

The above deductions are in good agreement with what was known about the deposit both from direct investigations (sampling and boreholes) and from laboratory analyses of the samples. This could mean an experimental confirmation that the nomogram in fig. 8 is substantially correct and useful. Therefore, SIP measurements can contribute significantly to the body of knowledge on the deposit, since information can be obtained from it on grain size and mineral content.

REFERENCES

ANDERSON, W.L. and B.D. SMITH (1986): Nonlinear least-squares inversion of frequency domain induced polarization (program NLSIP), USGS open-file report 86-280.

COLE, K.S. and R.H. COLE (1941): Dispersion and absorption in dielectrics, *J. Chem. Phys.*, **9,** 341-351.

GRILLO, S.M., F. MELIS, S. PRETTI, M. FIORI and G. SPIGA (1990): Some aspects of geochemical exploration in a new precious metal prospect in Sardinia, Italy, *Boll. Assoc. Min. Sub.*, **27** (4), 619-631.

JOHNSON, I.M. (1984): Spectral induced polarization parameters as determined through time-domain measurements, *Geophysics,* **49,** 1993-2003.

MAJOR, J. and J. SILIC (1981): Restrictions on the use of Cole-Cole dispersion models in complex resistivity interpretation, *Geophysics,* **46,** 916-931.

PELTON, W.H., P.G. HALLOF and R.J. SMITH (1972): *Parameters to Describe Second-Order IP Effects in the Frequency Domain* (McPhar Geophysics Ltd., Toronto).

PELTON, W.H., S.H. WARD, P.G. HALLOF, W.R. SILL and P.H. NELSON (1978): Mineral discrimination and removal of inductive coupling with multifrequency IP, *Geophysics,* **43,** 588-609.

SEIGEL, H.O. (1959): Mathematical formulation and type curves for induced polarization, *Geophysics,* **24,** 547-565.

SONG, L. and K. VOZOFF (1985): The complex resistivity spectra of models consisting of two polarizable media of different intrinsic properties, *Geophys. Prospect.*, **33,** 1029-1062.